



JOINT INSTITUTE FOR NUCLEAR RESEARCH

Dzhelepov Laboratory of Nuclear Problems

FINAL REPORT ON THE SUMMER STUDENT PROGRAM

*Planarity Analysis of the Micromegas
detector readout panels for the ATLAS
New Small Wheel upgrade project at
CERN*

Student:

Lisan D. Cabrera, Cuba,
Pinar del Rio University

Supervisor:

Dr. Alexi Gongadze

Participation period:

June 03 – July 23

Dubna, 2017

Abstract.

Presently, Micromegas chamber production line have been constructed at the Dzhelepov Laboratory of Nuclear Problems (DLNP) of the Joint Institute for Nuclear Research (JINR). Production line will provide production and testing of 64 Micromegas readout planes and 32 quadruplets for the outer part of LM2 large sectors of the ATLAS News Small Wheel.

The manufacturing process of these panels must follow a set of strict conditions in order to accomplish the establish requirements. One of these requirements is check that honeycomb sheet used for panel construction has 10 ± 0.05 mm of thickness. Another requirement is to ensure the enough surface planarity of the panels, task that is solved by optical probe fixed on the Computer Numerical Control (CNC) machine with help of some calibration measurements to obtain the surface topography. In order to know how surface of the vacuum tables affect planarity of the panels the distance between the vacuum tables along the entire surface during the assembly process was simulated. These measurements were analyzed with ROOT (CERN) and the results achieved were satisfactory.

Content

Introduction.....	1
NSW Micromegas structure.....	1
Results and discussion.....	3
• Thickness of the honeycomb sheet.....	3
• Simulated distance between the vacuum tables.....	3
• Surface and thickness of the LM2 readout panels.....	5
Conclusions.....	8
Acknowledgments.....	8
References.....	9

Introduction.

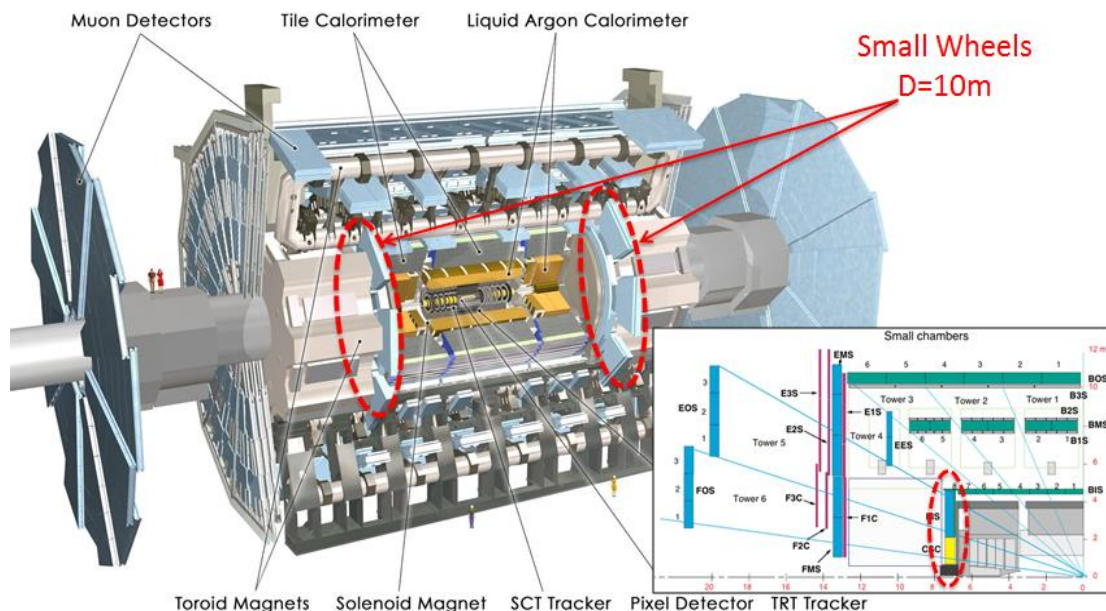
The Large Hadron Collider will be upgraded in several stages to increase the energy and the luminosity. Both increased luminosity and energy of the LHC will lead to a significant increase of radiation load of the elements of the ATLAS detector, first of all in regions close to the interaction point. One of such parts of the ATLAS detector is the so-called Small Wheel of the muon detector system. It is planned that it will be completely replaced by a New Small Wheel (NSW) during the Phase-1 upgrade (2019-2020). The Micromegas (MICRO MESH Gaseous Structure) and sTGC (small Thin Gap Chamber) were chosen both for trigger and tracking. The main coordinate detector will use Micromegas, and the trigger one will use the sTGC. The main requirements for the detectors are the following: operation at count rates of up to 15 kHz/cm^2 , excellent tracking capabilities, time resolution sufficient for particle identification and good resistance to aging.

The DLNP takes part in the mass production of Micromegas chambers to build the NSW [1]. The Institute's contribution is the production and testing of 64 double-sided readout panels, as well as the assembling and testing of 32 quadruplets (Fig. 2) with the drift panels produced at Aristotle University of Thessaloniki. Finally, all produced and tested chambers will be shipped to CERN.

One of the element to take into account in the production of these panels is the surface planarity requirement, this one should be known with root mean square error of less than $80 \text{ }\mu\text{m}$ [2] over 3 m^2 surface, which will be the main study subject in this work.

NSW Micromegas structure.

The NSW layout is constituted by small (SM) and large (LM) sector modules (Fig. 1). The DLNP is focused in the outer part of large sectors (LM2) readout panel mass production.



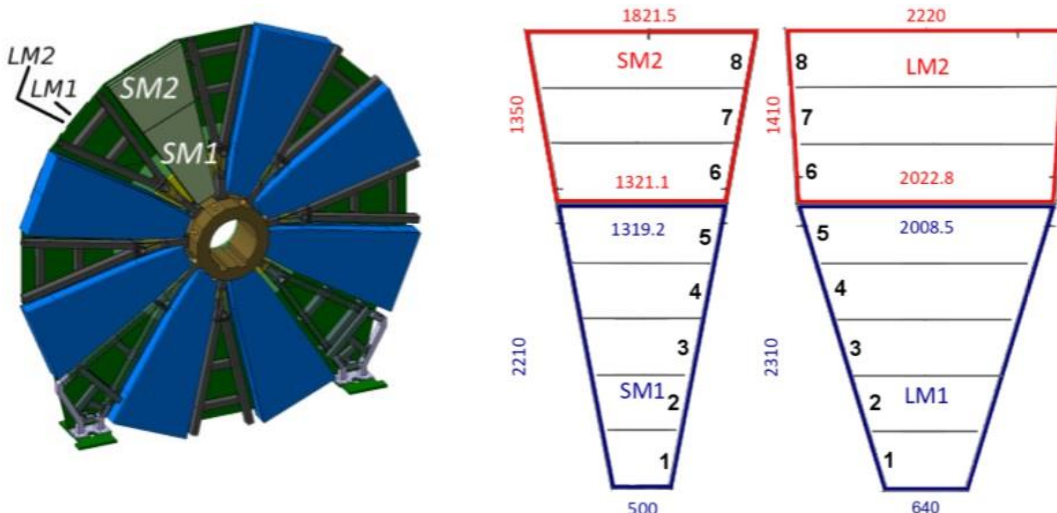


Fig. 1. The NSW in ATLAS experiment and its layout with the dimensions in millimeters

These sector modules have a quadruplet design to fit 5 panel layers in the planned 8 cm (Fig. 2). The quadruplet consists of three drifts and two double-sided readout panels [2]. A condition to work with a 100 μm spatial resolution is that the 1st and 2nd readout layers (Eta) are parallel to each other and perpendicular to the radial direction. In the case of the 3rd and 4th readout layers the inclination is $+1.5^\circ$ respecting to the Eta planes in one side of the second readout panel (Stereo) and -1.5° in the other side of the Stereo panel in order to know the coordinate perpendicular to the strip direction with the same precision as the two Eta parallel-strips layers [3]. More details in the panel gluing process and the quadruplet assembly are presented in [4] and [5]. The energy resolution for a 150 μm amplification gap is presented in [6] as well as a simple description of the fabrication process and assembly of the micromesh layer.

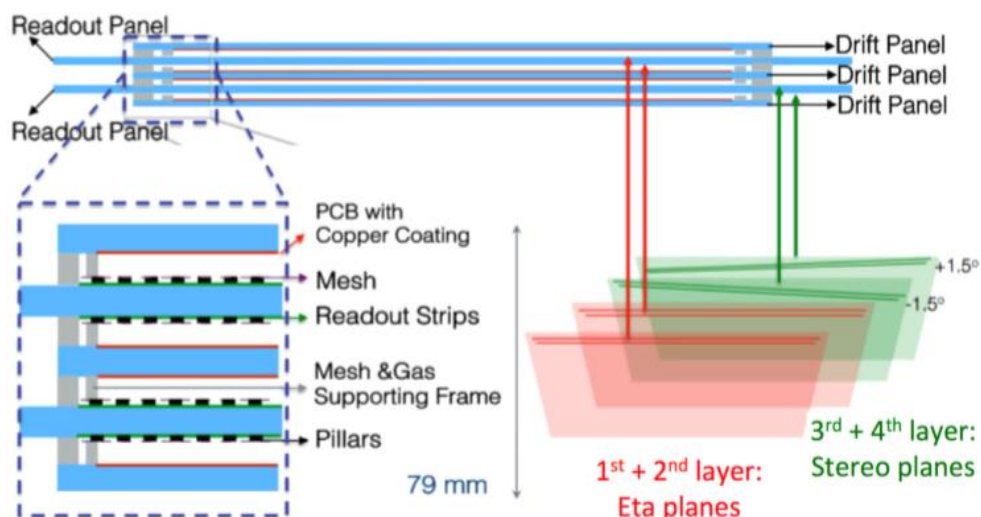


Fig. 2. Layout of the NSW quadruplet

Micromegas is a two stage parallel-plate detector invented by Giomataris et al. in 1996. It uses a thin metal mesh (micromesh) to separate the drift region where the primary electrons are produced from the amplification region where they are multiplied. The mesh is manufactured of different materials (nickel, copper, aluminum, stainless steel) and using different methods,

such as electroforming, chemical etching, weaving, deposition. The stainless steel woven mesh is used for NSW upgrade. The detector working gas is an Ar:CO₂ (93:7) gas mixture. The Fig. 3 [11] present the simplest model of the Micromegas detector functioning: the incoming radiation ionize the gas in the 5mm drift gap creating positive ions and electrons, these last ones move, due the applied electric field (0,6 kV/cm), to the mesh. When the electrons pass through the mesh they accelerate due the applied high electric field (40-45 kV/cm) between the metal mesh and anode strips, generating a cascade effect, and finally the electrons are collected by the anode strips [2].

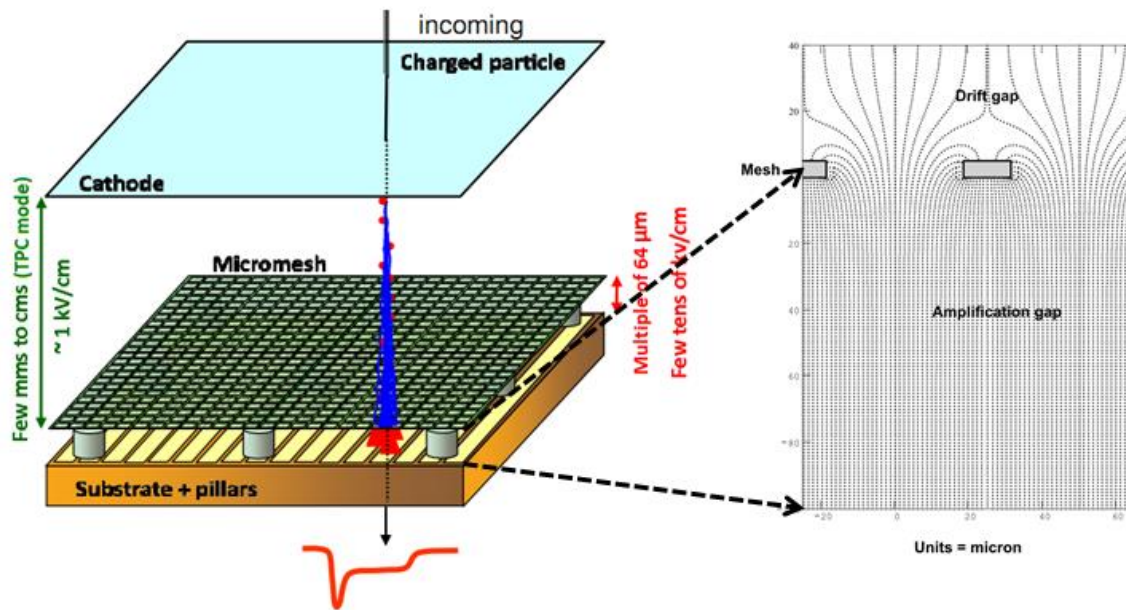


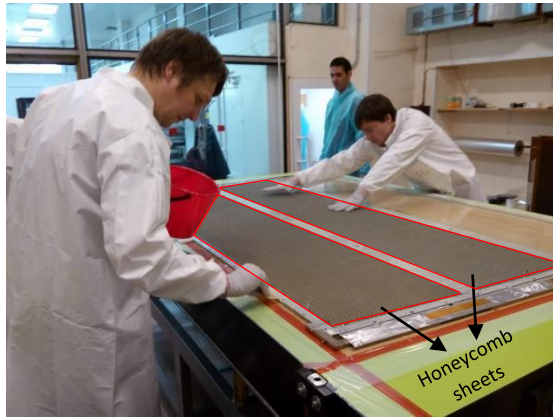
Fig. 3. Schematic view of a Micromegas detector and electric field map

In [9] is shown a more graphic description of the applied electric field in both, the drift and the amplification gaps. In [7] is found more information about this process and its simulation.

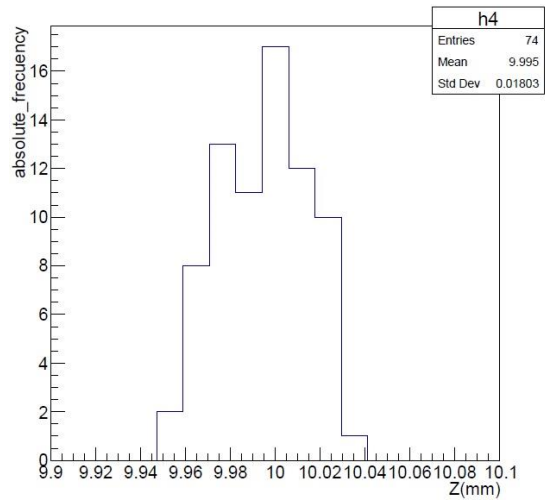
Results and discussion

Thickness of the honeycomb sheet.

In order to check the manufacturing quality of the components in the panel production the honeycomb sheet thickness (Fig.4a) was measured in equidistant spots along the panel. The expected thickness in all the grid should be (10 ± 0.05) mm [10] and [4]. The results are shown in Fig. 4b.



a. Readout panel assembly in the clean room of DLNP



b. Histogram of the total honeycomb sheets thickness

Fig. 4. Thickness checking of the honeycomb sheets

The histogram shows, as was thought, a mean thickness value of $\sim(10 \pm 0.02)$ mm, satisfying the requirements.

Simulated distance between the vacuum tables.

Is desired to simulate the thickness of the panels in the assembling process. For this purpose, an optical probe was used to obtain the surface topography of the vacuum tables (Fig 5). This optical probe is programed to measure with an X axis step of 11 mm, and with a Y axis step of 20 mm.

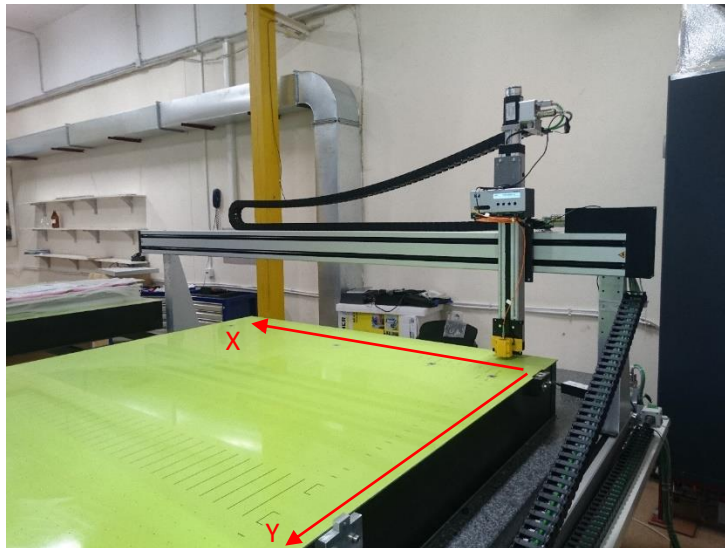
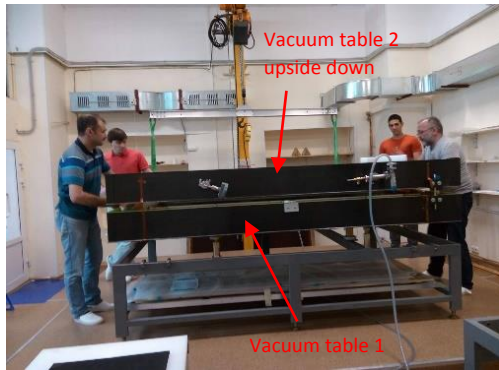
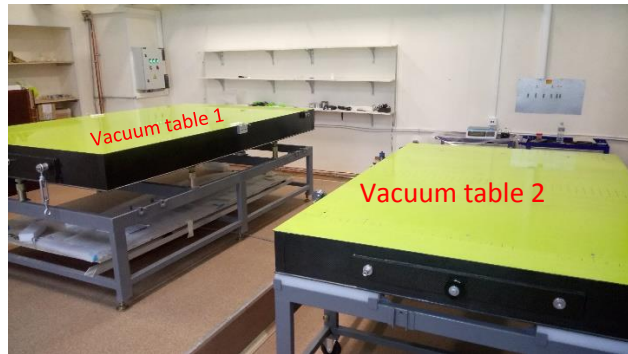


Fig. 5. The optical probe measurement process on the vacuum tables

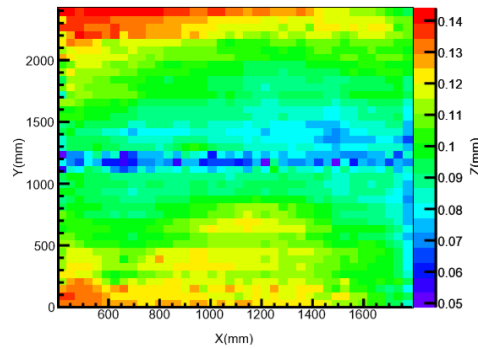
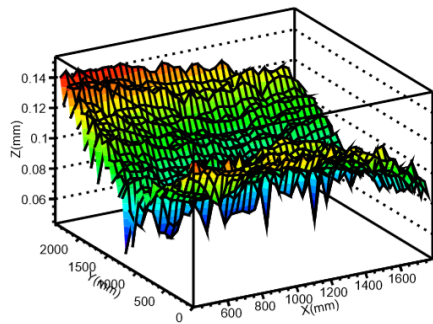
A calibration run was needed to obtain the surfaces shape. In the real construction process, the table 2 is put on the table 1, and then in the simulation is made the same procedure (Fig. 6).



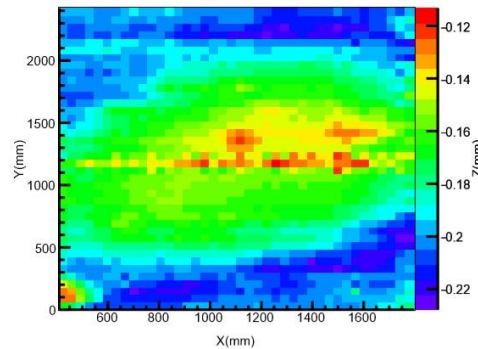
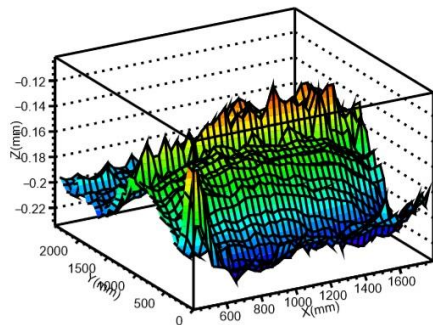
Simulation of the readout panel construction process



Vacuum tables



a. Surface shape of the vacuum table 1

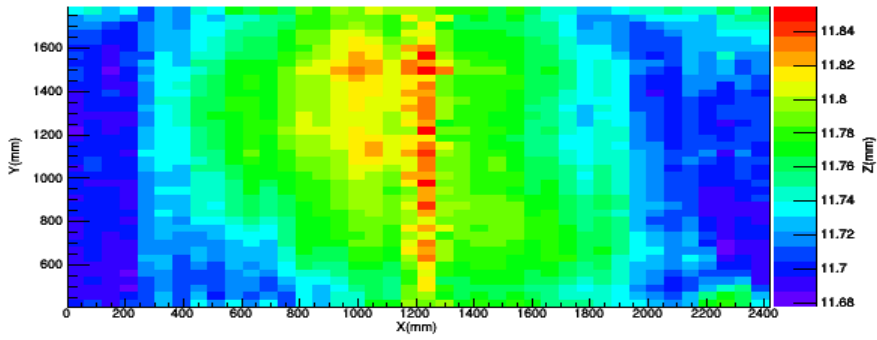


b. Surface shape of the vacuum table 2 upside down

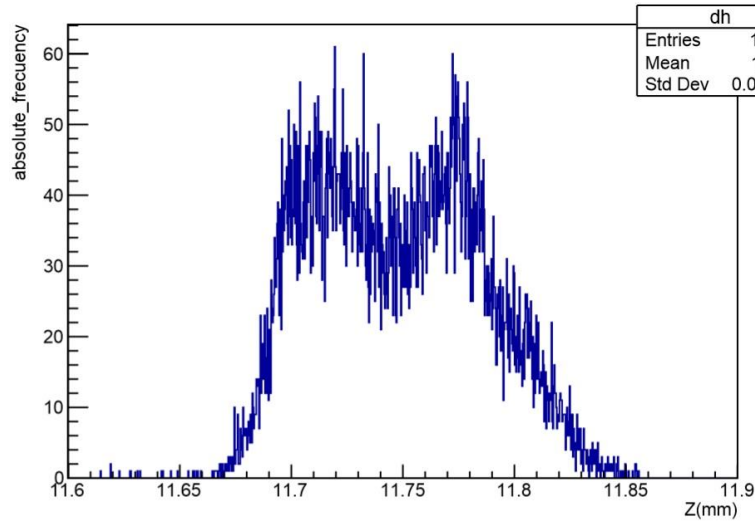
Fig. 6. Surface shape of the vacuum tables after rotation correction

The Z axis values in Fig. 6 are meaningless without calibration. The interest of the results shown in this figure is only for the surfaces shape. What is useful is the differences between these values in order to know the planarity deformation, which is within the requirements and have better value than the reported by [2].

Then, the use of precise shims of 11,7 mm thick located in certain points of the border allow to control the distance of the vacuum table 2 upon the 1, so the same procedure is simulated. The steps and its pictures in the assembly process of the readout panels and the quadruplet were presented by [8]. The distance difference of the tables was rotated $+90^\circ$ around the Z axis in order to compare these results with the surface of the panels. The final results of this analysis are shown in Fig. 7.



a. Simulation of the distance between the vacuum tables in the assembly process

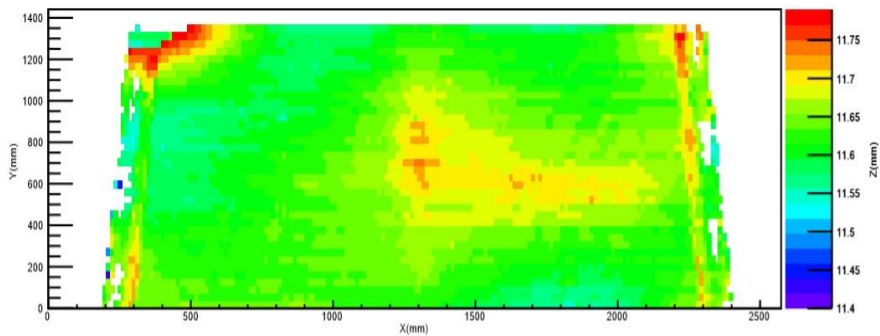


b. Histogram of the distance between the vacuum tables

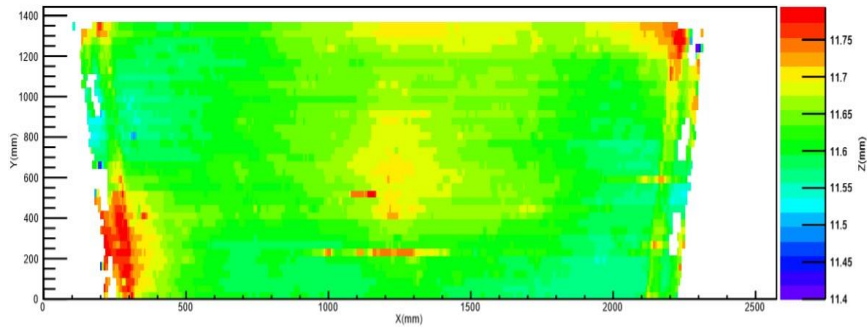
Fig. 7. Distance between the vacuum tables and it histogram

Surface and thickness of the LM2 readout panels.

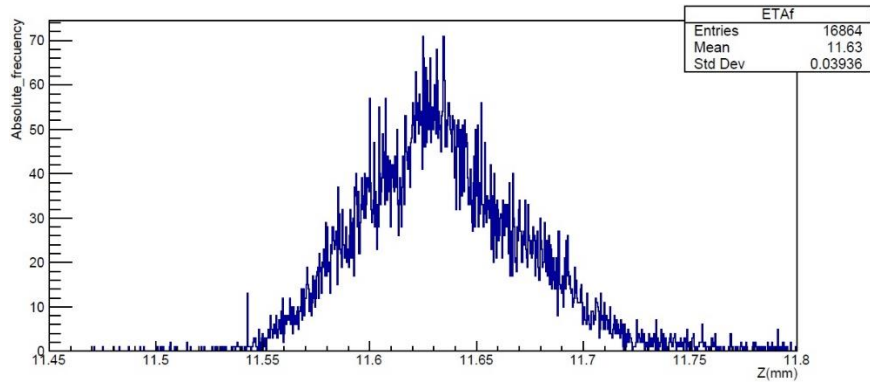
The same optical probe was used to measure the surface topography of the panels by both sides (front and back). A 11,6 mm thick shims was collocated near the panels in the measurement process for calibration purpose. The Fig. 8 and 9 present the Eta and Stereo panel height results correspondingly already calibrated.



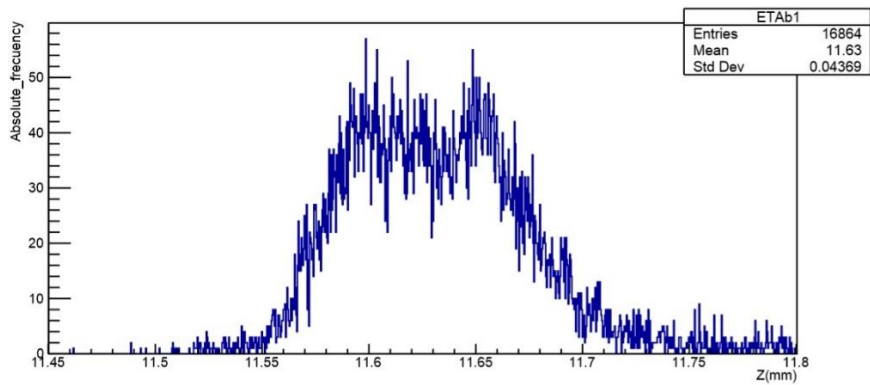
a. LM2 Eta readout panel front thickness



b. LM2 Eta readout panel back thickness

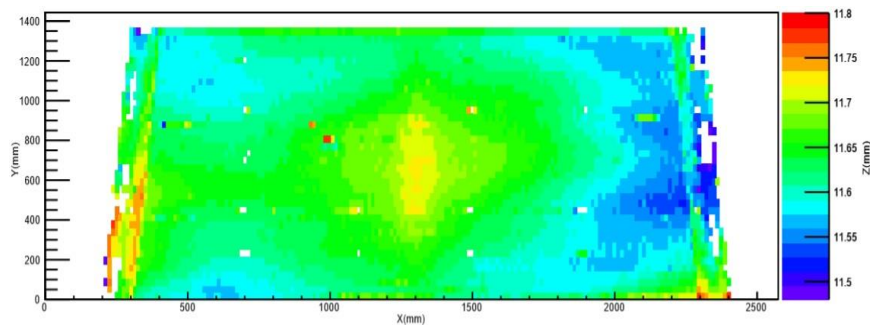


c. Histogram of the LM2 Eta readout panel front thickness

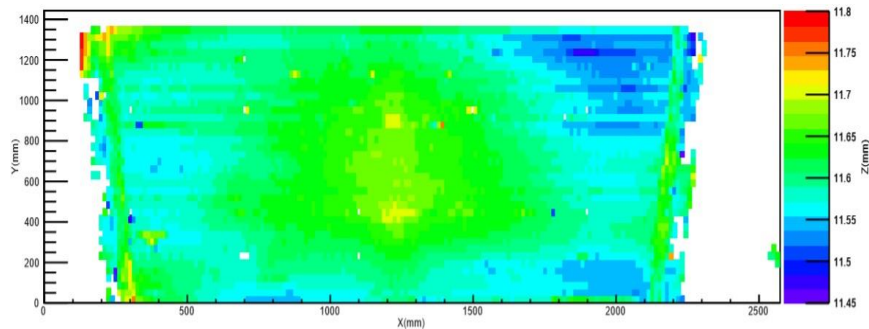


d. Histogram of the LM2 Eta readout panel back thickness

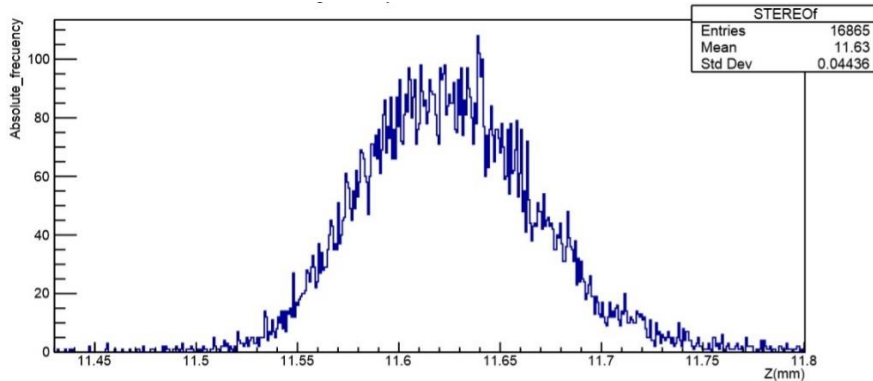
Fig. 8. Thickness results of the LM2 Eta readout panel



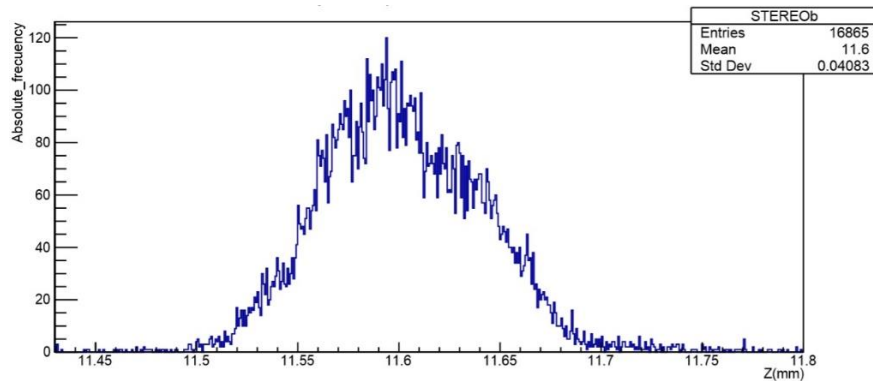
a. LM2 Stereo readout panel front thickness



b. LM2 Stereo readout panel back thickness



c. Histogram of the LM2 Stereo readout panel front thickness



d. Histogram of the LM2 Stereo readout panel back thickness

Fig. 9. Thickness results of the LM2 Stereo readout panel

As can be seen in the Fig. 8 and 9 the standard deviation in every case is less than 45 μm . The mean values and its standard deviations are presented in Tab. 1.

Tab. 1. Resume of the LM2 readout panels mean and standard deviation values

Readout panel side	Mean (mm)	Standard deviation (mm)
Eta front	11.6343	0.0394
Eta back	11.6328	0.0437
Stereo front	11.6254	0.0444
Stereo back	11.6017	0.0408

When the current and literature results are compared, is remarkable that all the planarity values obtained for the readout panels produced by the DLNP are superior than the reported in [2] ($\pm 50 \mu\text{m}$), so is correct to say that the our results are satisfactory.

Conclusions.

The NSW is made up of several Micromegas detectors structures, one of them: the LM2 readout panels are manufactured by the DLNP of the JINR, which has the duty to guarantee that panel's parameters are within requirements. The honeycomb sheet thickness was measured and the results is the one expected (10 ± 0.05 mm). Also, was studied the planarity of the readout panels, and the standard deviation achieved in the worst case (± 44.4 μm) is better compared to the presented in [2] (± 50 μm), being the best standard deviation reached result ± 39.4 μm . The distance between the tables was achieved, showing that the space between them in the assembly process has a standard deviation of ~ 37.6 μm , which is approximately equal to the planarity results of the readout panels, proving that the simulation process was correct.

Acknowledgments.

I want to give my greatest gratitude to my supervisor Dr. Alexi Gongadze for the orientations and for make possible this opportunity, as well as to Igor, Irma, Irakli, Rostislav, Tania, Dima and the other research members of the Micromegas collective for giving me this great laboratory experience, their help and friendships.

I also would like to express my most sincere gratitude to Dr. Antonio Leyva Fabelo for his guide and support during this stay, as well as to Dr. Alexei Zhemchugov, Mrs. Elena Karpova, and to the rest of the JINR University Center staff for all the managements.

Thanks to the DLNP for this research opportunity and financial support.

References.

- [1] JINR (2017) Micromegas chamber production starts at JINR in preparation for ATLAS upgrade. <http://www.jinr.ru/posts/micromegas-chamber-production-starts-at-jinr-in-preparation-for-atlas-upgrade/>.
- [2] Kruger F. (2016) Performance studies of resistive Micromegas detectors for the upgrade of the ATLAS Muon spectrometer. NIM A, vol. 845, pp. 248-252, <http://dx.doi.org/10.1016/j.nima.2016.06.006>.
- [3] ATLAS Collaboration (2013) New Small Wheel Technical Design Report. CERN –LHCC-2013-006, ATLAS – TDR-20-2013.
- [4] Bianco M., Danielsson H., Degrange J., De Olivera R., Farina E., Kuger F., Iengo P., Perez F., Sekhniaidze G., Sforza F., Sidiropoulou O., Vergain M., Wotshack J., Dudder A., Lin T. H., Schott M., Valderanis C. (2015) Construction of two large-size four-plane micromegas detectors. arXiv:1511.03884v1 [physics.ins-det].
- [5] Bortfeldt J. (2015) Construction and Test of Full-Size Micromegas Modules for the ATLAS New Small Wheel Upgrade. 4th International Conference on Micro Pattern Gaseous Detectors, Ludwig-Maximilians-University Munich, Germany.
- [6] Giomataris I., De Olivera R., Andriamonje S., Aune S., Charpak G., Colas P., Fanourakis G., Ferrer E., Giganon A., Rebourgeard Ph., Salin P. (2006) Micromegas in a bulk. NIM A, vol. 560, pp. 405-408, doi: 10.1016/j.nima.2005.12.222.
- [7] Brickwedde B., Dudder A., Schott M., Yildirim E. (2016) Design, Construction and Performance Test of a Prototype MicroMegas Chamber with Two Readout Planes in Common Gas Volume. arXiv:1610.09539v1 [physics.int-det].
- [8] Iodice M. (2016) Resistive Micromegas for the Muon Spectrometer Upgrade of the ATLAS Experiment. ICHEP 2016, Chicago USA.
- [9] Giomataris Y. (1998) Development and prospects of the new gaseous detector "Micromegas". NIM A, vol. 419, pp. 239-250, PII: S0168-9002(98)00865-1.
- [10] Iodice M., Gongadze A., Kharchenko D., Jeanneau F., Temming K., Bini C., Introzzi G., Gaudio G., Hertenberger R., Dudder A., Klitzner F., Lampoudis C., Giraud J., Peyaud A., Sampsonidis D., Paschalias P. (2017) Quality Control during NSW micromegas construction and acceptance criteria, ATLAS Project Document No. ATL-M-QP-XXX v.1
- [11] Gongadze A. L. (2016) Micromegas Chambers for the Experiment ATLAS at the LHC (A Brief Overview), Physics of Particles and Nuclei, vol. 47, no. 2, pp. 270–289.